Crystal Plasticity

R. J. Asaro
Division of Engineering,
Brown University,
Providence, R.I. 02912

Significant progress has been made during the past decade in incorporating micromechanics in continuum descriptions of inelastic deformation. This has led to the development of a rather comprehensive constitutive theory for rate-dependent and idealized rate-independent crystalline materials that deform plastically by crystalline slip. This theory is reviewed in some detail and examples are presented which illustrate how complex slip phenomena involving localized plastic flow and nonuniform crystallographic texture can be analyzed. The paper concludes by suggesting that it is now possible to develop accurate models for rate-dependent polycrystals undergoing arbitrarily large strains. Such models would have as principal aims the prediction of texture development and the rigorous assessment of such anisotropy on constitutive behavior. An example of how this would be of immediate value in analyzing strain-hardening behavior of metal polycrystals at large strains is provided.

1 Introduction

This paper has four main objectives. The first is to provide a very brief overview of some important aspects of crystalline plasticity, especially of features that are important for the development of large strain-continuum constitutive laws. The second is to illustrate how these features can be included in a continuum framework. In meeting these objectives our attention is nearly confined to describing the kinematics of crystalline slip; a somewhat detailed overview of dislocation mechanics as it relates to constitutive laws can be found in other recent reviews [1, 2]. The third goal is to show that, when some of the salient micromechanical features are included in continuum analyses of large strain plasticity of crystalline solids, accurate and perhaps surprisingly detailed descriptions of complex slip phenomena are obtained. Examples are given of nonuniform deformation in crystals which illustrate the vital role played by crystal lattice kinematics and, in particular, of the development of crystallographic texture. The final objective is to suggest how these analyses could be extended to develop models for large strain, rate-dependent, polycrystalline behavior. There is indeed a clear and strong impetus for this which is illustrated in connection with strain-hardening phenomena in metals at large strains. Essentially what is proposed as a useful direction for future research is the development of a large strain theory and suitable models for polycrystals that would extend those originally proposed by G. I. Taylor in 1938 [3] to describe deformation texture. As discussed in Section 4, the theory required to accomplish this would have to be rate-dependent so that lattice kinematics is described unambiguously.

The detailed plan of the paper is as follows. In Section 2 the basic kinematics of crystalline slip is cast in a rigorous framework and constitutive laws are presented for rate-independent and rate-dependent crystalline materials. The kinematical structure here falls within the framework laid out by Hill and Rice [3] and is confined to deformation by crystallographic dislocation slip alone; in the present paper we do not consider deformation by twinning, diffusion, or grain boundary sliding, for example. The constitutive theory is placed within a more general plasticity framework in Section 2. In Section 3 a set of complex slip phenomena known to be very important in the large strain deformation of single crystals and of individual grains of polycrystals is analyzed. The need for brevity demands that this be done using the rate-independent version of the theory although the examples are also used to highlight some inherent limitations of rate independence in accounting for what are obviously dominant lattice kinematical effects. References to recent rate-dependent analyses that overcome these fundamental problems of the rate-independent theory are provided. The success the analysis of Section 3 has in describing slip phenomena and the effects of nonuniform crystallographic texture on localized deformation should provide encouragement for a successful extension of the theory to the large strain deformation of polycrystals. In Section 4 this extension is proposed.

Standard notations are used throughout. Matrices and tensors, the rank and order of which are indicated in the text, are written in boldface type. The summation convention is used for Latin indices but summations over crystallographic slip systems are indicated explicitly. For brevity dots and double dots are used to indicate the following products:

$$\mathbf{P}\cdot\mathbf{n} = P_{ij}n_j,\ \mathbf{P}:\mathbf{D} = P_{ij}D_{ji}$$

and

$$\mathfrak{L}:\mathbf{P} = \mathfrak{L}_{ijkl}P_{lk},\ \boldsymbol{\sigma}\cdot\mathbf{P} = \sigma_{ij}P_{jk}$$

Other special symbols are defined in the text as needed.

Contributed by the Applied Mechanics Division for publication in the JOURNAL OF APPLIED MECHANICS.
Discussion on this paper should be addressed to the Editorial Department, ASME, United Engineering Center, 345 East 47th Street, New York, N.Y. 10017, and will be accepted until two months after final publication of the paper itself in the JOURNAL OF APPLIED MECHANICS. Manuscript received by ASME Applied Mechanics Division, April, 1983.

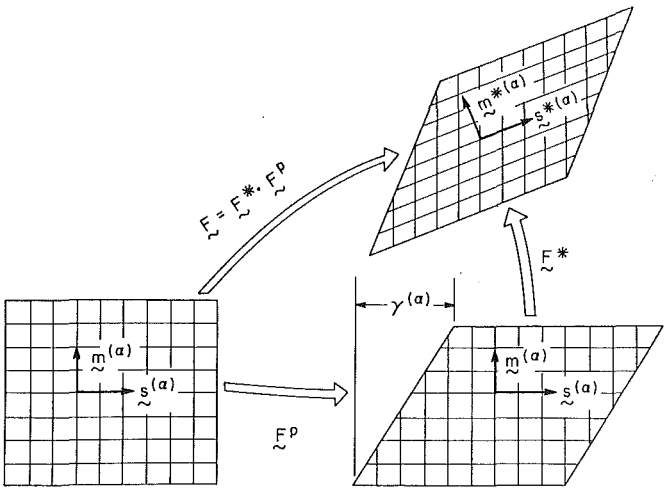

Fig. 1 Kinematics of elastic-plastic deformation of crystalline solid deforming by crystallographic slip

2 Constitutive Laws

2.1 Kinematics. A comprehensive kinematical theory for the mechanics of elastic-plastic deformation of crystals is now well established, at least when crystallographic slip is the sole cause of inelastic deformation. The development traces its origins to the pioneering work of Taylor [3] and to the precise mathematical expression of the physical concepts by Hill [5] and Hill and Rice [4]. In the following summary we will closely follow the procedures and the specific kinematical representation used by Asaro and Rice [6] and more recently by Peirce, Asaro, and Needleman [7, 8]. This particular scheme is chosen because of its clarity and utility in the analysis of boundary value problems.

A basic tenet of all the cited analyses is that material flows through the crystal lattice via dislocation motion as proposed by Taylor [3], whereas the lattice itself, with the material embedded on it, undergoes elastic deformations and rotations. The picture for this as shown by Asaro and Rice [6] and Peirce et al. [7] is given in Fig. 1. If $\mathbf{F}^P$ is the part of the total deformation gradient due solely to slip then the total deformation gradient, $\mathbf{F}$, is given by

$$\mathbf{F} = \mathbf{F}^* \cdot \mathbf{F}^P. \tag{2.1}$$

$\mathbf{F}^*$ is the lattice contribution to $\mathbf{F}$ and is associated with stretching and rotation of the lattice. The deformation gradient remaining after elastic unloading *and upon returning the lattice to its orientation in the reference state is* $\mathbf{F}^{*-1} \cdot \mathbf{F} = \mathbf{F}^P$. Of course, in real processes removal of the loads alone will not return the lattice to its original state and thus what remains as a residual $\mathbf{F}$ after slip is more than just $\mathbf{F}^P$; the lattice may be permanently reoriented (but undeformed) for example, as well as placed in a state of residual deformation.

As the crystal deforms and rotates, lattice vectors stretch and rotate, i.e., they convect with the lattice. The slip direction and other vectors lying in the slip plane can be taken to be such vectors. When this is done, the slip direction $\mathbf{s}^{(\alpha)}$ of slip system α is given in the deformed configuration by

$$\mathbf{s}^{*(\alpha)} = \mathbf{F}^* \cdot \mathbf{s}^{(\alpha)}. \tag{2.2}$$

The normal to the slip plane however, since it is normal to all vectors in the slip plane, is the reciprocal base vector corresponding to $\mathbf{m}^{(\alpha)}$ or

$$\mathbf{m}^{*(\alpha)} = \mathbf{m}^{(\alpha)} \cdot \mathbf{F}^{*-1}. \tag{2.3}$$

$\mathbf{s}^{(\alpha)}$ and $\mathbf{m}^{(\alpha)}$ are taken to be unit vectors that define the slip system α in the reference state. $\mathbf{s}^{*(\alpha)}$ and $\mathbf{m}^{*(\alpha)}$ are not in general unit vectors, but remain orthogonal since $\mathbf{s}^{*(\alpha)} \cdot \mathbf{m}^{*(\alpha)} = \mathbf{s}^{(\alpha)} \cdot \mathbf{m}^{(\alpha)} = 0$.

The velocity gradient in the current state is given by a standard formula:

$$\mathbf{L} = \dot{\mathbf{F}} \cdot \mathbf{F}^{-1} = \dot{\mathbf{F}}^* \cdot \mathbf{F}^{*-1} + \mathbf{F}^* \cdot \dot{\mathbf{F}}^P \cdot \mathbf{F}^{P-1} \cdot \mathbf{F}^{*-1} \tag{2.4}$$

where $\mathbf{L}$ can also be expressed as

$$\mathbf{L} = \mathbf{D} + \boldsymbol{\Omega}. \tag{2.5}$$

$\mathbf{D}$ and $\boldsymbol{\Omega}$ are the symmetric rate of stretching and spin tensors, respectively; in terms of the velocity $\mathbf{v}$ and spatial coordinates $\mathbf{x}$ their components are given by

$$D_{ij} = 1/2(\partial v_i/\partial x_j + \partial v_j/\partial x_i) \tag{2.6}$$

and

$$\Omega_{ij} = 1/2(\partial v_i/\partial x_j - \partial v_j/\partial x_i). \tag{2.7}$$

$\mathbf{D}$ and $\boldsymbol{\Omega}$ may be decomposed from (2.4) into plastic parts ($\mathbf{D}^P$, $\boldsymbol{\Omega}^P$) and lattice parts ($\mathbf{D}^*$ and $\boldsymbol{\Omega}^*$) as follows:

$$\mathbf{D} = \mathbf{D}^* + \mathbf{D}^P, \quad \boldsymbol{\Omega} = \boldsymbol{\Omega}^* + \boldsymbol{\Omega}^P \tag{2.8}$$

where

$$\mathbf{D}^P + \boldsymbol{\Omega}^P = \mathbf{F}^* \cdot \dot{\mathbf{F}}^P \cdot \mathbf{F}^{P-1} \cdot \mathbf{F}^{*-1}. \tag{2.9}$$

Since in our present discussion plastic deformation occurs by dislocation slip, we find in the current state that

$$\mathbf{D}^P + \boldsymbol{\Omega}^P = \sum_{\alpha=1}^{n} \dot{\gamma}^{(\alpha)} \mathbf{s}^{*(\alpha)} \mathbf{m}^{*(\alpha)} \tag{2.10}$$

where $\dot{\gamma}^{(\alpha)}$ is the slipping rate of the α slip system and is defined relative to the reference state lattice, i.e., $\dot{\gamma}^{(\alpha)}$ are *defined* so that

$$\dot{\mathbf{F}}^P \cdot \mathbf{F}^{P-1} = \sum_{\alpha=1}^{n} \dot{\gamma}^{(\alpha)} \mathbf{s}^{(\alpha)} \mathbf{m}^{(\alpha)}.$$

In (2.10) and in what follows the sum ranges over all slip systems that participate in the deformation increment.

Finally, we note that the plastic parts of the rate of stretching and the rate of spin are given by the symmetric and skew parts of (2.10). It is convenient to introduce for each slip system the tensors $\mathbf{P}^{(\alpha)}$ and $\mathbf{W}^{(\alpha)}$ defined as

$$\mathbf{P}^{(\alpha)} = 1/2(\mathbf{s}^{*(\alpha)} \mathbf{m}^{*(\alpha)} + \mathbf{m}^{*(\alpha)} \mathbf{s}^{*(\alpha)}) \tag{2.11}$$

and

$$\mathbf{W}^{(\alpha)} = 1/2(\mathbf{s}^{*(\alpha)} \mathbf{m}^{*(\alpha)} - \mathbf{m}^{*(\alpha)} \mathbf{s}^{*(\alpha)}). \tag{2.12}$$

Then, from (2.10)

$$\mathbf{D}^P = \sum_{\alpha=1}^{n} \mathbf{P}^{(\alpha)} \dot{\gamma}^{(\alpha)} \tag{2.13}$$

and

$$\boldsymbol{\Omega}^P = \sum_{\alpha=1}^{n} \mathbf{W}^{(\alpha)} \dot{\gamma}^{(\alpha)}. \tag{2.14}$$

2.2 Constitutive Laws. We will assume that the crystal's elasticity is unaffected by slip, then following Hill and Rice [4] the elastic law takes the form

$$\overset{\nabla}{\boldsymbol{\tau}}{}^* = \underset{\sim}{\mathcal{L}} : \mathbf{D}^* \tag{2.15}$$

where $\underset{\sim}{\mathcal{L}}$ is the tensor of elastic moduli and $\overset{\nabla}{\boldsymbol{\tau}}{}^*$ is the Jaumann rate of Kirchoff stress. We will for the present discussion consider $\underset{\sim}{\mathcal{L}}$ to be derivable from a potential (free energy) function so that it possesses symmetry in the leading and trailing indices. Here the superscript * signifies that the derivative is of the stress components formed on axes that rotate with the *lattice* and so according to the standard formula,

$$\overset{\nabla}{\tau}{}^{*} = \dot{\tau} - \Omega^{*} \cdot \tau + \tau \cdot \Omega^{*} \tag{2.16}$$

where $\dot{\tau}$ is the material rate of Kirchoff stress. This, in turn, is defined as $\rho_0/\rho\sigma$ where σ is Cauchy stress and ρ_0 and ρ are the mass densities in the reference and current states. To formulate constitutive laws for the material we introduce the Jaumann stress rate on axes that rotate with the material,

$$\overset{\nabla}{\tau} = \dot{\tau} - \Omega \cdot \tau + \Omega \cdot \tau \tag{2.17}$$

and note by using (2.14) that the difference between these two stress rates is

$$\overset{\nabla}{\tau}{}^{*} - \overset{\nabla}{\tau} = \sum_{\alpha=1}^{n} \beta^{(\alpha)} \dot{\gamma}^{(\alpha)} \tag{2.18}$$

where

$$\beta^{(\alpha)} = \mathbf{W}^{(\alpha)} \cdot \tau - \tau \cdot \mathbf{W}^{(\alpha)}. \tag{2.19}$$

By combining (2.13), (2.14), (2.15), and (2.19) we obtain the constitutive law

$$\overset{\nabla}{\tau} = \underset{\sim}{\mathcal{L}} : \mathbf{D} - \sum_{\alpha=1}^{n} [\underset{\sim}{\mathcal{L}} : \mathbf{P}^{(\alpha)} + \beta^{(\alpha)}] \dot{\gamma}^{(\alpha)} \tag{2.20}$$

where it remains to specify the shearing rates $\dot{\gamma}^{(\alpha)}$ in terms of stress or stress rate.

Now before proceeding with the development of the $\dot{\gamma}$'s for rate-independent and then rate-dependent materials we introduce a particular definition of the so-called resolved shear stress, or *Schmid stress* for a slip system. Essentially this is a component of shear stress resolved in the slip plane and in the slip direction and thus is the component of stress that produces forces on dislocations causing them to slip. With this in mind it should be noted that this stress is caused not only by macroscopically applied loads but also by elastic interactions with other dislocations or misfitting defects. Asaro and Rice [6] have discussed various ways this definition can be made but, as noted by Rice [11], there is one particular definition that we call the Schmid stress with which basic notions such as the existence of plastic potentials and normality structure to flow laws (when these exist) are most concisely phrased. This is the Schmid stress, $\tau^{(\alpha)}$, defined to be work conjugate to the $\dot{\gamma}^{(\alpha)}$ such that $\tau^{(\alpha)} \dot{\gamma}^{(\alpha)}$ is precisely the rate of working due to slip on system α per unit *reference* volume. Then from the general expression for this rate of working,

$$\tau : \mathbf{D}^{P} = \sum_{\alpha=1}^{n} \tau : \mathbf{P}^{(\alpha)} \dot{\gamma}^{(\alpha)} \tag{2.21}$$

we identify

$$\tau^{(\alpha)} = \mathbf{P}^{(\alpha)} : \tau. \tag{2.22}$$

For rate-independent materials, flow laws (as prescribed later) adapted from the well-known Schmid law of a "critical resolved shear stress" connect the rate of slipping on each slip system to the rates of change of the $\tau^{(\beta)}$. Some useful expressions for $\dot{\tau}^{(\alpha)}$ are given in the following. For rate-dependent materials, simple kinetic laws for dislocation motion, again adapted from Schmid's law, generally relate the slipping rates on each slip system to the resolved shear stress itself. When the stress dependence of the slip rates in both cases involves only $\tau^{(\alpha)}$, and precisely the $\tau^{(\alpha)}$ as defined, normality rules can be shown to result. This essential structure for both time-dependent and independent constitutive laws has been discussed at length by Hill [9], Rice [10, 11], and Hill and Rice [12]. Because of its obvious importance for future developments of constitutive models for polycrystalline flow a very brief statement of normality rules for crystals is given in the next section. The promised expressions for $\dot{\tau}^{(\alpha)}$ are however given first.

It is important to note that since the $\mathbf{P}^{(\alpha)}$ depend on lattice orientation and stress state, they change during a program of loading and straining – if the material stresses were cycled for instance, so that plastic flow occurred and the lattice rotated relative to the material before the stresses were returned to their original values, the $\mathbf{P}^{(\alpha)}$ would undergo a permanent change. A general expression for $\dot{\tau}^{(\alpha)}$ can then be given in terms of the material time derivatives of $\mathbf{P}^{(\alpha)}$ and τ

$$\dot{\tau}^{(\alpha)} = \dot{\mathbf{P}}^{(\alpha)} : \tau + \mathbf{P}^{(\alpha)} : \dot{\tau} \tag{2.23}$$

or from either of the two corotational derivatives introduced previously, namely,

$$\dot{\tau}^{(\alpha)} = \overset{\nabla}{\mathbf{P}}{}^{*}(\alpha) : \tau + \mathbf{P}^{(\alpha)} : \overset{\nabla}{\tau}{}^{*} \tag{2.24}$$

and

$$\dot{\tau}^{(\alpha)} = \overset{\nabla}{\mathbf{P}}{}^{(\alpha)} : \mathrm{z} + \mathbf{P}^{(\alpha)} : \overset{\nabla}{\tau}. \tag{2.25}$$

Now it is easy to verify that, when the deformation is only elastic,

$$\overset{\nabla}{\mathbf{P}}{}^{*(\alpha)} : \tau = \beta^{(\alpha)} : \mathbf{D}^{*} \tag{2.26}$$

and that $\dot{\tau}^{(\alpha)}$ may also be computed from

$$\dot{\tau}^{(\alpha)} = \mathbf{P}^{(\alpha)} : \overset{\nabla}{\tau}{}^{*} + \beta^{(\alpha)} : \mathbf{D}^{*} \tag{2.27}$$

or, after using (2.15), from

$$\dot{\tau}^{(\alpha)} = (\mathbf{P}^{(\alpha)} : \underset{\sim}{\mathcal{L}} + \beta^{(\alpha)}) : \mathbf{D}^{*}. \tag{2.28}$$

The last relation will be useful in what follows for understanding the nature of the normality rules that follow from the Schmid stress.

2.3 Normality Rules and Plastic Potentials. In this section a very brief discussion is given of the origins of normality and the kinetic restrictions that lead to the existence of plastic potentials. As mentioned earlier, a concise and elegant framework for this has been given by Hill and Rice [12] and what follows is a short summary of their results. Where appropriate, however, certain quantities are identified using the specific kinematical description given in Sections 2.1 and 2.2 and this should provide a helpful link for the reader in making contact with the Hill and Rice work.

Inelastic materials are considered that are capable of exhibiting purely elastic response at any stage in the deformation history. For rate-independent, elastic-plastic materials such a purely elastic response results when stress variations are directed and terminate within the current yield surface, the existence of which would also be assumed. For rate-dependent materials, on the other hand, the response may be purely elastic only when the stress variations are very rapid compared to the fastest rates at which inelastic slip processes can respond. The scope of this framework would seem to encompass a wide range of crystallographic slip processes occurring at quasi-static strain rates and perhaps even at strain rates of up to 10^3.

Now again following Hill and Rice [12], let $\mathbf{e}$ denote any objective, symmetric strain tensor and let $\mathbf{t}$ be its work conjugate (symmetric) stress defined in the manner laid out by Hill [13]. As in (2.21) then, $\tau : d\mathbf{e}$ is an increment of work per unit reference volume, that is, per unit volume in the reference state from where $\mathbf{e}$ is measured. If $\mathbf{e}$ is taken to be the Green strain, for example,

$$\mathbf{e}^{G} = 1/2(\mathbf{F}^{T} \cdot \mathbf{F} - \mathbf{I}),$$

and then $\mathbf{t}$ is the Piola-Kirchoff stress

$$\mathbf{t}^{G} = \mathbf{F}^{-1} \cdot \tau \cdot \mathbf{F}^{-1T}.$$

To draw a correspondence with the specific kinematical schemes of Sections 2.1 and 2.2 it is useful to also consider the logarithmic strain measure defined as

$$\mathbf{e}^{0} = ln(\mathbf{\Lambda}) = (\mathbf{\Lambda} - \mathbf{I}) - \frac{1}{2}(\mathbf{\Lambda} - \mathbf{I})^{2} + \ldots$$

(provided no principal stretch exceeds 2) where the stretch tensor $\mathbf{\Lambda}$ is defined by writing $\mathbf{F} = \mathbf{R}\cdot\mathbf{\Lambda}$ where $\mathbf{R}$ is a pure rotation. Hill [14] has shown, with a derivation not reproduced here, that the objective conjugate stress to this measure can be expressed as

$$\mathbf{t}^0 = |\mathbf{F}|\mathbf{R}^T\cdot\boldsymbol{\sigma}\cdot\mathbf{R} + \mathcal{O}(e^2)$$

where $\boldsymbol{\sigma}$ is the Cauchy stress. Then if the current state and reference states are taken to be coincident, all stress measures equal $\boldsymbol{\sigma}$, and all strain rates equal $\mathbf{D}$ and $\overset{\circ}{t}{}^0 = \overset{\nabla}{\tau}$.

The inelasticity in our restricted class of solids is thought to occur as a result of a (enormously complex) set of microstructural rearrangements, e.g., as a result of the incremental motion of large numbers of dislocation segments. At each stage the current dislocated state of the material is denoted symbolically by H and the properties of the solid are a functional of this prior history. Furthermore if the material's response is assumed to be of Green type in the sense that a potential (i.e., free energy) exists for all dislocated states, then the following can be taken to hold for any purely *elastic* strain variation $\delta\mathbf{e}$ at fixed H ($dH \neq 0$ implies dislocation slips and the accumulation of plastic strain)

$$\mathbf{t}:\delta\mathbf{e} = \delta\phi(\mathbf{e}, H) \tag{2.29}$$

and

$$\mathbf{t} = \frac{\partial\phi}{\partial\mathbf{e}} = \mathbf{t}(\mathbf{e}, H). \tag{2.30}$$

In the foregoing we use the symbolism introduced by Hill and Rice [12] that variations indicated by a δ are purely elastic; this, of course, means that $\delta H = 0$. The free energy function $\phi(\mathbf{e}, H)$ depends on the dislocated state through the self and interaction energies of the assumed internal variables, e.g., the dislocation segments. A dual potential can be introduced via the Legendre transformation

$$\psi = \mathbf{t}:\mathbf{e} - \phi \tag{2.31}$$

and as before, for a purely elastic variation, we find

$$\mathbf{e}:\delta\mathbf{t} = \delta\psi(\mathbf{e}, H) \tag{2.32}$$

and

$$\mathbf{e} = \frac{\partial\psi}{\partial\mathbf{t}}. \tag{2.33}$$

At this point we reintroduce the fourth-order tensor of elastic moduli $\underset{\sim}{\mathcal{L}}$ and its inverse $\underset{\sim}{\mathcal{L}}^{-1}$ here defined for the pair $(\mathbf{t}, \mathbf{e})$. If $d\mathbf{e}$ is an arbitrary strain variation, $\underset{\sim}{\mathcal{L}}:d\mathbf{e}$ is the stress increment that *would* result if the response *were* purely elastic. When the response is elastic-plastic, however, $d\mathbf{t}$ is the actual stress increment, and the difference

$$d^P\mathbf{t} = d\mathbf{t} - \underset{\sim}{\mathcal{L}}:d\mathbf{e} = d\mathbf{t} - \frac{\partial\mathbf{t}}{\partial\mathbf{e}}:d\mathbf{e} \tag{2.34}$$

is what Hill and Rice have called the "plastic" part of the increment. In the same manner, $\underset{\sim}{\mathcal{L}}^{-1}:d\mathbf{t}$ is the strain increment that *would* result from purely elastic response and the difference

$$d^P\mathbf{e} = d\mathbf{e} - \underset{\sim}{\mathcal{L}}^{-1}:d\mathbf{t} = d\mathbf{e} - \frac{\partial\mathbf{e}}{\partial\mathbf{t}}:d\mathbf{t} \tag{2.35}$$

is the "plastic part." These two plastic quantities are related by the elastic moduli

$$d^P\mathbf{t} = -\underset{\sim}{\mathcal{L}}:d^P\mathbf{e} \quad \text{and} \quad d^P\mathbf{e} = -\underset{\sim}{\mathcal{L}}^{-1}:d^P\mathbf{t}. \tag{2.36}$$

It is observed from (2.34) and (2.35) that for a rate-independent material $d^P\mathbf{t}$ is the residual change (decrement) in stress after an infinitesimal cycle of $\mathbf{e}$ during which inelastic straining occurs, whereas $d^P\mathbf{e}$ is the residual increment of plastic strain during an infinitesimal loading-unloading cycle of $\mathbf{t}$.

The "plastic parts" as defined in the foregoing can be easily identified for the specific kinematical representation given in Section 2.1 and Section 2.2. If t denotes time, dt a time increment, we identify $d\mathbf{t}$ and $d\mathbf{e}$ as

$$d\mathbf{t} \Leftrightarrow \overset{\nabla}{\tau}\, dt \tag{2.37$_1$}$$

and

$$d\mathbf{e} \Leftrightarrow \mathbf{D}\, dt \tag{2.37$_2$}$$

then examining (2.20) we identify

$$d^P\mathbf{t} \Leftrightarrow (\overset{\nabla}{\tau}\, dt)^P = -\sum_{\alpha=1}^{n} \{\underset{\sim}{\mathcal{L}}:\mathbf{P}^{(\alpha)} + \boldsymbol{\beta}^{(\alpha)}\} d\gamma^{(\alpha)} \tag{2.38$_1$}$$

and

$$d^P\mathbf{e} \Leftrightarrow (\mathbf{D}dt)^P = \sum_{\alpha=1}^{n} \{\mathbf{P}^{(\alpha)} + \underset{\sim}{\mathcal{L}}^{-1}:\boldsymbol{\beta}^{(\alpha)}\} d\gamma^{(\alpha)} \tag{2.38$_2$}$$

where $d\gamma^{(\alpha)} = \dot{\gamma}^{(\alpha)}\, dt$.

It is informative to identify these "plastic parts" explicitly since it is the plastic increment $(\mathbf{D}dt)^P$ which can be shown, with appropriate kinetic assumptions, to be normal to the yield surface in stress space and not

$$\mathbf{D}^P dt \left(= \sum_{\alpha=1}^{n} P^{(\alpha)} d\gamma^{(\alpha)}\right)$$

defined earlier in (2.8), (2.10), and (2.13).

The plastic parts of the increments in free energies are similarly defined by Hill and Rice [12] as

$$d^P\phi = \phi(\mathbf{e}, H + dH) - \phi(\mathbf{e}, H) \tag{2.39}$$

and

$$d^P\psi = \psi(\mathbf{t}, H + dH) - \psi(\mathbf{t}, H). \tag{2.40}$$

Furthermore as pointed out by them, the potentials, ϕ and ψ, and thus the increments, can be evaluated at any $\mathbf{e}$ or $\mathbf{t}$ where ϕ and H are defined. Then if $d^P\phi$ and $d^P\psi$ are differentiated with respect to $\mathbf{e}$ and $\mathbf{t}$, respectively, we find from (2.30) and (2.33) that

$$\frac{\partial}{\partial\mathbf{e}}(d^P\phi) = \mathbf{t}(\mathbf{e}, H + dH) - \mathbf{t}(\mathbf{e}, H) = d^P\mathbf{t} \tag{2.41}$$

and

$$\frac{\partial}{\partial\mathbf{t}}(d^P\psi) = \mathbf{e}(\mathbf{t}, H + dH) - \mathbf{e}(\mathbf{t}, H) = d^P\mathbf{e} \tag{2.42}$$

which effectively shows that the plastic variations in the potentials serve as potentials for the plastic parts of variations in stress and strain. To identify these latter potentials and demonstrate the fundamental role played by the Schmid stress we first examine the question of normality. This is done with respect to conjugte variables.

Normality for Rate-Independent Materials. At each history a yield surface is supposed to exist in either $\mathbf{t}$ or $\mathbf{e}$ space. Confining our attention to $\mathbf{t}$ space, suppose the current stress is at a point on the yield surface where dH occurs producing a plastic increment $d^P\mathbf{e}$. If $\delta\mathbf{t}$ represents *any* stress increment beginning at this stress point but directed *inside*, and if

$$\delta\mathbf{t}:d^P\mathbf{e} < 0 \tag{2.43}$$

for all such $\delta\mathbf{t}$'s, then the strain increment will be said to be normal. Further implications regarding the behavior of the potential ϕ itself are seen by studying the Il'yushin inequality for a strain cycle involving an infinitesimal plastic strain increment, viz,

$$\oint \mathbf{t}:d\mathbf{e} \geq 0. \tag{2.44}$$

The integral is taken about a strain cycle beginning at a point within the yield surface and the inequality holds if plastic strain occurs. To evaluate this integral, carry out the three segment cycle suggested by Hill and Rice: (*a*) from an arbitrary point interior to the yield surface at strain $\mathbf{e}_o$, load (elastically) to the yield point at strain $\mathbf{e}_y$; (*b*) load elastic-plastically to the strain $\mathbf{e}_y + d\mathbf{e}_y$ (on the subsequent yield surface characterized by $H + dH$), and unload elastically within the *new elastic domain* back to $\mathbf{e}_y$; and finally (*c*) unload back to $\mathbf{e}_o$ elastically. The final segment can be taken along the same path in (*a*) because of the assumed path independence within elastic domains. Segment (*b*) contributes a second-order effect and thus may be ignored. Furthermore by appealing to (2.30) we note that along segment (*a*) $\mathbf{t} = \mathbf{t}(\mathbf{e}, H)$ while along (*b*) with the same end points, $\mathbf{t} = \mathbf{t}(\mathbf{e}, H + dH)$. It is evident then that by using (2.41),

$$\oint \mathbf{t}:d\mathbf{e} = \int_{\mathbf{e}_o}^{\mathbf{e}_y} \{\mathbf{t}(\mathbf{e}, H) - \mathbf{t}(\mathbf{e}, H+dH)\}:\delta\mathbf{e} =$$

$$-\int_{\mathbf{e}_o}^{\mathbf{e}_y} d^P\mathbf{t}:\delta\mathbf{e} = -\int_{\mathbf{e}_o}^{\mathbf{e}_y} \frac{\partial}{\partial \mathbf{e}}(d^P\phi):\delta\mathbf{e} = d^P\phi\Big|_{\mathbf{e}_y}^{\mathbf{e}_o}. \tag{2.45}$$

The Il'yushin postulate when applied to such cycles thus states that

$$d^P\phi\Big|_{\mathbf{e}_y}^{\mathbf{e}_o} \geq 0. \tag{2.46}$$

To see how this singles out the Schmid stress in connection with normality, consider the following heuristic construct. If ϕ is the isothermal Hemholtz free energy per unit reference volume, $d^P\phi$ is its change at *fixed overall strain* due to the occurrence of slips $d\gamma^{(\alpha)}$. If $\tau^{(\alpha)}$ is the *net* Schmid stress produced by applied loads *and interactions with the dislocated state* (characterized by H) then

$$\sum_{\alpha=1}^{n} \tau^{(\alpha)} d\gamma^{(\alpha)}$$

is the work done through the slips and

$$-\sum_{\alpha=1}^{n} \tau^{(\alpha)} d\gamma^{(\alpha)}$$

is the change in ϕ. Of course this is equivalent to identifying $\tau^{(\alpha)}$ as the thermodynamic force acting on a set of internal variables whose infinitesimal variations are identified with the $d\gamma^{(\alpha)}$'s which, incidentally, is an alternative starting point for defining $\tau^{(\alpha)}$ (Rice [11] in fact starts from that point). Then combining (2.44) and (2.46) the Il'yushin postulate applied to such cycles becomes for the case of crystallographic slip

$$\oint \mathbf{t}:d\mathbf{e} = \sum_{\alpha=1}^{n} (\tau_y^{(\alpha)} - \tau^{(\alpha)})\, d\gamma^{(\alpha)} \geq 0. \tag{2.47}$$

where τ_y is evaluated at $\mathbf{e}_y$ on the yield surface and $\tau^{(\alpha)}$ at *any* point within the surface. In fact (2.43) implies that if $d\gamma^{(\alpha)} > 0$, for example, $\delta\tau^{(\alpha)} < 0$, for any $\delta\mathbf{t}$ variation emanating from a yield point since, by (2.28) and the fact that $\delta\mathbf{t} = \underset{\sim}{\mathfrak{L}}:\delta\mathbf{e}$ for elastic variations,

$$\delta\mathbf{t}:d^P\mathbf{e} = \sum_{\alpha=1}^{n} \{\mathbf{P}^{(\alpha)}:\underset{\sim}{\mathfrak{L}} + \boldsymbol{\beta}^{(\alpha)}\}:\delta\mathbf{e}\; d\gamma^{(\alpha)} = \sum_{\alpha=1}^{n} \delta\tau^{(\alpha)} d\gamma^{(\alpha)} < 0 \tag{2.48}$$

at least whenever at least one $d\gamma^{(\alpha)} \neq 0$; in deriving (2.48) we note that $\delta\mathbf{e} = \mathbf{D}^* dt$ for this purely elastic variation. If the flow laws or hardening rules are such that each pair $\delta\tau^{(\alpha)} d\gamma^{(\alpha)} < 0$ when $\dot{\tau}^{(\alpha)}$ is *changed elastically*, normality follows. This is true when the yield surface is smooth or when the stress point is at a corner made up of intersecting yield planes.

Rate-Dependent Materials. Still following Hill and Rice, we consider materials that exhibit elastic response to sufficiently rapid loading or straining and take a constitutive law in the form

$$\frac{d^P\mathbf{e}}{dt} = \frac{d\mathbf{e}}{dt} - \mathfrak{L}^{-1}:\frac{d\mathbf{t}}{dt} \tag{2.49}$$

Here $d^P\mathbf{e}/dt$ is thought to depend on the current state of stress and dislocated state but instantaneous stress changes are met with the assumed purely elastic response. Thus it is possible to examine variations of the type $\delta\mathbf{t}:d^P\mathbf{e}/dt$ and if this is a perfect differential, say

$$\delta\mathbf{t}:\frac{d^P\mathbf{e}}{dt} = \delta\Gamma(\mathbf{t}, H) \tag{2.50}$$

then

$$\frac{d^P\mathbf{e}}{dt} = \frac{\partial\Gamma}{\partial\mathbf{t}} \tag{2.51}$$

and a flow potential exists. For the present case of crystallographic slip we take $\delta\mathbf{t}$ to be $\underset{\sim}{\mathfrak{L}}:\mathbf{D}^*\delta t = \underset{\sim}{\mathfrak{L}}:\delta\mathbf{e}$ and use the identity (2.38_2) for $d^P\mathbf{e}$ to obtain

$$\sum_{\alpha=1}^{n} \{\mathbf{P}^{(\alpha)}:\underset{\sim}{\mathfrak{L}} + \boldsymbol{\beta}^{(\alpha)}\}\delta\mathbf{e}\frac{d\gamma^{(\alpha)}}{dt} \tag{2.52}$$

which can be rewritten as

$$\sum_{\alpha=1}^{n} \delta\tau^{(\alpha)} \frac{d\gamma^{(\alpha)}}{dt} \tag{2.53}$$

Now, as Rice [10, 11] has suggested, if the kinetic laws for $d\gamma^{(\alpha)}/dt$ are stress-dependent only through the associated conjugate force $\tau^{(\alpha)}$, equation (2.53) is a perfect differential and a flow potential and normality again result.

2.4 Hardening Laws for Rate-Independent Materials. In this section hardening laws are formulated in accordance with the normality rules described in the preceding section. This is done using the kinematical representation introduced in Sections 2.1 and 2.2. Two quantities for each slip system are first defined:

$$\boldsymbol{\lambda}^{(\alpha)} = \mathbf{P}^{(\alpha)}:\underset{\sim}{\mathfrak{L}} + \boldsymbol{\beta}^{(\alpha)} \tag{2.54}$$

and

$$\boldsymbol{\mu}^{(\alpha)} = \mathbf{P}^{(\alpha)} + \underset{\sim}{\mathfrak{L}}^{-1}:\boldsymbol{\beta}^{(\alpha)} = \underset{\sim}{\mathfrak{L}}^{-1}:\boldsymbol{\lambda}^{(\alpha)} \tag{2.55}$$

Consistent with the normality structure just described we state that plastic flow occurs on slip system α when $\tau^{(\alpha)}$ reaches a critical value $\tau_c^{(\alpha)}$. For those so-called "critical systems" where $\tau^{(\alpha)} = \tau_c^{(\alpha)}$

$$\dot{\tau}^{(\alpha)} = \dot{\tau}_c^{(\alpha)} = \sum_{\beta=1}^{n} h_{\alpha\beta}\dot{\gamma}^{(\beta)} \quad \text{if } \dot{\gamma}^{(\alpha)} > 0 \tag{2.56}$$

which maintains $\tau^{(\alpha)}$ at the current yield value.

If the system becomes inactive

$$\dot{\tau}^{(\alpha)} \leq \dot{\tau}_c^{(\alpha)} = \sum_{\beta=1}^{n} h_{\alpha\beta}\dot{\gamma}^{(\beta)} \quad \text{with } \dot{\gamma}^{(\alpha)} = 0. \tag{2.57}$$

For noncritical systems there is only the inequality

$$\tau^{(\alpha)} < \tau_c^{(\alpha)} \quad \text{with } \dot{\gamma}^{(\alpha)} = 0. \tag{2.58}$$

The $h_{\alpha\beta}$ are the slip-plane hardening rates; the diagonal terms represent "self-hardening" on a slip system whereas the off-diagonal terms represent coupled or "latent hardening." The effect of latent hardening is described in Section 2.6 where some of its implications are compared to experiments.

When these relations are combined with (2.54), (2.55), and (2.28), the hardening laws take the form

$$\boldsymbol{\lambda}^{(\alpha)}:\mathbf{D}^* = \boldsymbol{\mu}^{(\alpha)}:\overset{\nabla}{\boldsymbol{\tau}}{}^* = \sum_{\beta=1}^{n} h_{\alpha\beta}\dot{\gamma}^{(\beta)}, \quad \dot{\gamma}^{(\alpha)} > 0 \tag{2.59}$$

and

$$\boldsymbol{\lambda}^{(\alpha)}:\mathbf{D}^* = \boldsymbol{\mu}^{(\alpha)}:\overset{\nabla}{\boldsymbol{\tau}}{}^* \leq \sum_{\beta=1}^{n} h_{\alpha\beta}\dot{\gamma}^{(\beta)}, \quad \dot{\gamma}^{(\beta)} > 0 \tag{2.60}$$

In terms of the total material deformation rate **D** we find after using (2.8)

$$\boldsymbol{\lambda}^{(\alpha)}:\mathbf{D} = \sum_{\beta=1}^{n} g_{\alpha\beta}\dot{\gamma}^{(\beta)}, \quad \dot{\gamma}^{(\beta)} > 0 \tag{2.61}$$

$$\boldsymbol{\lambda}^{(\alpha)}:\mathbf{D} \leq \sum_{\beta=1}^{n} g_{\alpha\beta}\dot{\gamma}^{(\beta)}, \quad \dot{\gamma}^{(\alpha)} = 0 \tag{2.62}$$

or in terms of the material Jaumann rates $\overset{\nabla}{\boldsymbol{\tau}}$

$$\boldsymbol{\mu}^{(\alpha)}:\overset{\nabla}{\boldsymbol{\tau}} = \sum_{\beta=1}^{n} k_{\alpha\beta}\dot{\gamma}^{(\beta)}, \quad \dot{\gamma}^{(\alpha)} > 0 \tag{2.63}$$

$$\boldsymbol{\mu}^{(\alpha)}:\overset{\nabla}{\boldsymbol{\tau}} \leq \sum_{\beta=1}^{n} k_{\alpha\beta}\dot{\gamma}^{(\beta)}, \quad \dot{\gamma}^{(\alpha)} > 0. \tag{2.64}$$

The matrices **g** and **k** were introduced in this context by Hill and Rice [4] and for the specific kinematical description used here the elements are given by

$$g_{\alpha\beta} = h_{\alpha\beta} + \boldsymbol{\lambda}^{(\alpha)}:\mathbf{P}^{(\beta)} \tag{2.65}$$

and

$$k_{\alpha\beta} = h_{\alpha\beta} - \boldsymbol{\mu}^{(\alpha)}:\boldsymbol{\beta}^{(\beta)}. \tag{2.66}$$

These two matrices play a particularly significant role regarding "slip mode" uniqueness as shown by Hill and Rice. The details are not reproduced here but their main result, which takes the form of sufficiency conditions, is simply stated: when the **D**'s are fully specified the specification of the $\dot{\gamma}^{(\alpha)}$'s is unique if **g** is positive-definite; if the stress rates are instead specified, in our case the $\overset{\nabla}{\boldsymbol{\tau}}$'s, uniqueness is guaranteed if **k** is positive-definite. It should be noted that the restrictions placed on material properties such as latent hardening to insure uniqueness of the slip mode are rather severe and in fact too restrictive to include the full range of experimentally observed behavior. This will be discussed a bit further in connection with a specific model study later.

If, however, **g** can be inverted (2.61) yields

$$\dot{\gamma}^{(\alpha)} = \sum_{\beta=1}^{n} g^{-1}_{\alpha\beta}\boldsymbol{\lambda}^{(\beta)}:\mathbf{D} \tag{2.67}$$

and

$$\overset{\nabla}{\boldsymbol{\tau}} = \mathbf{C}:\mathbf{D} \tag{2.68}$$

with

$$\mathbf{C} = \underset{\sim}{\mathcal{L}} - \sum_{\alpha=1}^{n}\sum_{\beta=1}^{n} \boldsymbol{\lambda}^{(\alpha)} g^{-1}_{\alpha\beta}\boldsymbol{\lambda}^{(\alpha)}. \tag{2.69}$$

2.5 Kinetic Laws for Rate-Dependent Materials. The formulation of suitable kinetic laws for dislocation motion has received much attention and suitable reviews of the subject are available. For the present we will confine our attention to isothermal behavior and to quasi-static strain rates.

The specific law we adopt here for purposes of subsequent calculatoin is the simple power law used earlier by Hutchinson [15] for polycrystalline creep and by Pan and Rice [16] to describe the influence of rate sensitivity on yield vertex behavior in single crystals, viz,

$$\dot{\gamma}^{(\alpha)} = \dot{a}^{(\alpha)}\left(\frac{\tau^{(\alpha)}}{g^{(\alpha)}}\right)\left|\frac{\tau^{(\alpha)}}{g^{(\alpha)}}\right|^{(1/m)-1}. \tag{2.70}$$

Strain hardening is described by the evolution of the functions $g^{(\alpha)}$ which describe the current strain-hardened state. For example, Pan and Rice [16] propose the hardening law

$$\dot{g}^{(\alpha)} = \sum_{\beta=1}^{n} h_{\alpha\beta}\dot{\gamma}^{(\beta)} \tag{2.71}$$

where the $h_{\alpha\beta}$ are again slip-plane hardening moduli. As in the rate-independent theory, $h_{\alpha\alpha}$ represent self-hardening where $h_{\alpha\beta}\,(\alpha \neq \beta)$ are the latent hardening rates. $\dot{a}^{(\alpha)}$ has the simple interpretation of being reference strain rate on system α so that, for example, if $\dot{\gamma}^{(\alpha)} = \dot{a}^{(\alpha)}$ throughout the deformation history, $\tau^{(\alpha)} = g_0^{(\alpha)} + \int \dot{g}^{(\alpha)}\,dt$ where the integral is, of course, path dependent. In practice the $g^{(\alpha)}$ functions would be fit to τ versus γ curves obtained from single crystal deformed so that only one slip system was active, i.e., in a mode of "single slip;" the latent hardening rates are more

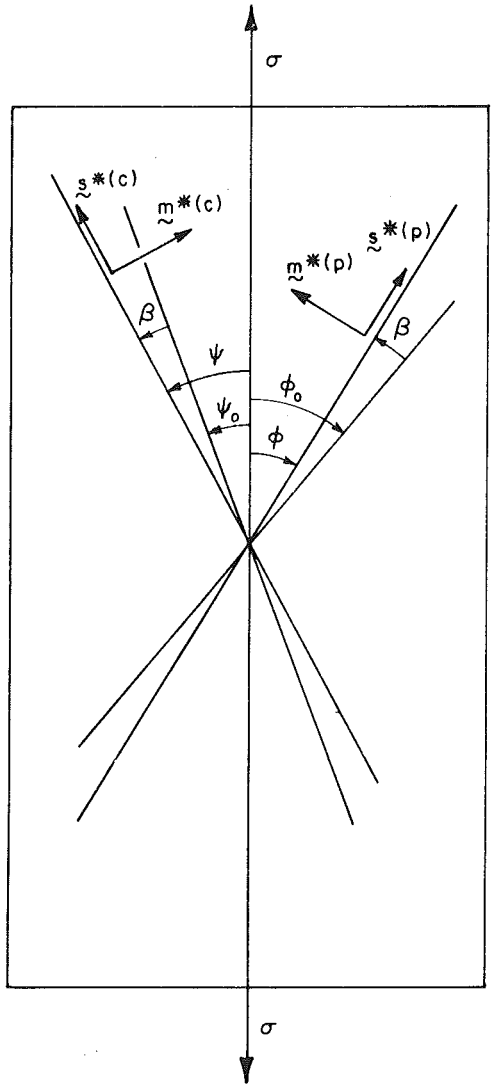

Fig. 2 Planar model for a single crystal subjected to tension. The crystal initially undergoes primarily single slip on the "primary" system labeled (p). Lattice rotations occur, designated by β, such that s(p) rotates toward the tensile axis which eventually causes the conjugate system to become active.

difficult to directly measure and are instead typically inferred via the effects they have on "overshoot" behavior as described in the next section.

In rate-dependent formulations of this type, there is no explicit yielding; all systems are active with the rate of shearing determined by (2.70). However, in practice, for values of $m \leq 0.02$ which incorporates a wide range of metal strain-rate sensitivities, "yielding" would appear to occur abruptly as $\tau^{(\alpha)}$ approaches the current value of $g^{(\alpha)}$; when $\tau^{(\alpha)} < g^{(\alpha)}$ the corresponding $\dot{\gamma}^{(\alpha)}$ is exceedingly small. Furthermore, using (2.70) in its present form does not require defining $(\mathbf{s}^{(\alpha)}, \mathbf{m}^{(\alpha)})$ and $(\mathbf{s}^{(\alpha)}, -\mathbf{m}^{(\alpha)})$ as different systems since negative $\dot{\gamma}^{(\alpha)}$'s are allowed. When this is done, however, the hardening law (2.71) would need to be altered so that inadvertent strain-softening effects are excluded. If Bauschanger effects were excluded outright, $\dot{\gamma}^{(\beta)}$ could be replaced with its absolute magnitude to yield an acceptable hardening law.

2.6 Latent Hardening. The slip-plane hardening rates $h_{\alpha\beta}$ introduced in (2.56) and (2.71) play a vital role in determining the character of the governing equations and therefore the patterns of deformation that develop at large strains. In addition, the level of latent hardening is of paramount importance in deciding whether or not the slip mode is unique in the rate-independent idealization of crystalline slip. The discussion, in fact, will show that the range of latent hardening observed in metals is such that uniqueness is perhaps only rarely guaranteed in a rate-independent model and is so only for simple crystal geometries involving relatively few slip systems. This would seem to place a severe limitation on the use of rate-independent theories since, as the examples given in Section 3 will show, large strain-deformation behavior in crystals depends intimately on lattice kinematics and therefore on the slip mode.

There are two methods which have appeared in the literature for estimating latent hardening. These have been reviewed recently by Peirce, Asaro, and Needleman [7], and Asaro [2] and so only a brief summary is given here. The first method involves deforming large crystals oriented for single slip and then cutting from them smaller specimens oriented for *single* slip on previously latent systems. The yield stress on the latent system is then compared to the flow stress of the original, or "primary," system. A second method is illustrated in Fig. 2. It is well known that when a single crystal is deformed in tension in single slip the lattice rotates relative to the loading axis such that the slip direction rotates *toward* the loading axis. The model sketched in Fig. 2 is meant to represent a cubic metal such as a face-centered or body-centered cubic metal and indicates that after a finite amount of slip on one system a second slip system eventually becomes equally stressed. This is known as the "conjugate" system. If slip is rate-independent and the hardening is isotropic such that all the $h_{\alpha\beta}$ are equal, we expect the conjugate system to yield when it becomes symmetrically oriented with respect to the primary system about the tensile axis. If the latent hardening rate of the conjugate slip system is larger than the self-hardening rate of the primary system, the lattice rotation "overshoots" the symmetry position until the resolved stress on the conjugate system exceeds that on the primary and conjugate slip begins. Measurements of the amount of overshoot therefore provide a means of estimating latent hardening levels. The two methods just described do not in general yield identical estimates of latent hardening. For one thing the strain path histories accumulated during the two tests are quite different and it is almost assured that the $h_{\alpha\beta}$ will be strongly path-dependent. For cases where loading produces multiple slip, estimates based on overshoot may be more representative and so we close this section with a brief discussion of overshoot observations and predictions.

Overshoot angles of between 0 and 4 deg have been commonly reported whereas there are cases of where secondary (i.e., conjugate) slip has been reported to begin even before symmetry positions are reached. Kocks [17] has reviewed much of this data and has summarized it by estimating that the ratio of latent hardening to self-hardening rates is between 1 to 1.4. For systems that share the same plane, this ratio is closer to 1 whereas for systems with intersecting planes the ratio is generally larger than unity. What is then important is that the hardening law used fits this range of observation. In the remainder of this section several hardening laws proposed in the literature are summarized and the implications they have for overshoot are explored in one particular case for rate-dependent and rate-independent materials.

As discussed by Peirce et al. [7], most of the hardening laws proposed to date process the symmetry $h_{\alpha\beta} = h_{\beta\alpha}$. For example, Hutchinson [18], Asaro [2], and Peirce et al. [7] have used the simple form

$$h_{\alpha\beta} = h_1 + (h - h_1)\delta_{\alpha\beta}. \tag{2.72}$$

This may be further simplified by setting $h_1 = qh$ where q is constant; the experimental range of q as suggested by Kocks [17] is then $1 \leq q \leq 1.4$. Symmetry of the $h_{\alpha\beta}$, however, generally implies a lack of symmetry in the matrix $\mathbf{g}$ and in the constitutive matrix $\mathbf{C}$. Symmetry in the matrix $\mathbf{C}$ allows the governing equations to be cast in variational form which is, in the rate-independent theory, very useful analytically. For example, in finite element calculations of the type performed by Peirce et al. [7] symmetry in $\mathbf{C}$ leads to symmetry in the global stiffness matrix. In addition, the variational structure imparted allows questions of uniqueness and bifurcation in boundary value problems to be addressed within the framework laid out by Hill [19]. Havner and Shalaby [20] recognized advantages of such symmetry and proposed a hardening law of the form

$$h_{\alpha\beta} = \mathcal{H}_{\alpha\beta} + \mathbf{P}^{(\alpha)} : \boldsymbol{\beta}^{(\beta)} \tag{2.73}$$

where in their "simple theory" $\mathcal{H}_{\alpha\beta}$ is taken to be symmetric and all the elements equal to $\mathcal{H}$. This law leads to very strong latent hardening via the coupling of the off-diagonal elements to stress through the $\boldsymbol{\beta}$'s which was used by them to describe overshoot. Peirce et al. [7] used a law with the form

$$h_{\alpha\beta} = \mathcal{H}_{\alpha\beta} + 1/2[\mathbf{P}^{(\alpha)} : \boldsymbol{\beta}^{(\beta)} - \boldsymbol{\beta}^{(\alpha)} : \mathbf{P}^{(\beta)}] \tag{2.74}$$

with $\mathcal{H}_{\alpha\beta} = \mathcal{H}_{\beta\alpha}$ but with the off-diagonal elements different than the diagonal elements; specifically they set

$$\mathcal{H}_{\alpha\beta} = q\mathcal{H} + (1 - q)\ \mathcal{H}\ \delta_{\alpha\beta} \tag{2.75}$$

as suggested in the foregoing. In the rate-dependent formulation of the type just described, on the other hand, the variational structure that follows from a symmetric $\mathbf{C}$ is not directly applicable and so it is just as convenient to simply specify the $h_{\alpha\beta}$ directly.

Peirce et al. [7] have carried out overshoot calculations using the plane model shown earlier in Fig. 2 for both rate-dependent and rate-independent calculations. In both cases the self-hardening rates took the form

$$h(\gamma) = h_0\ \mathrm{sech}^2 \left| \frac{h_0 \gamma}{\tau_s - \tau_0} \right| \tag{2.76}$$

where h_0 is the initial hardening rate, τ_0 is the yield stress, and γ is the cumulative shear strain on both slip systems, i.e.,

$$\gamma = \sum_{\beta=1}^{2} |\gamma^{(\alpha)}|.$$

This hardening rule describes a material that saturates at large strains as the flow stress approaches τ_s. In the rate-dependent case τ_0 is equal to $g^{(\alpha)}(0)$.

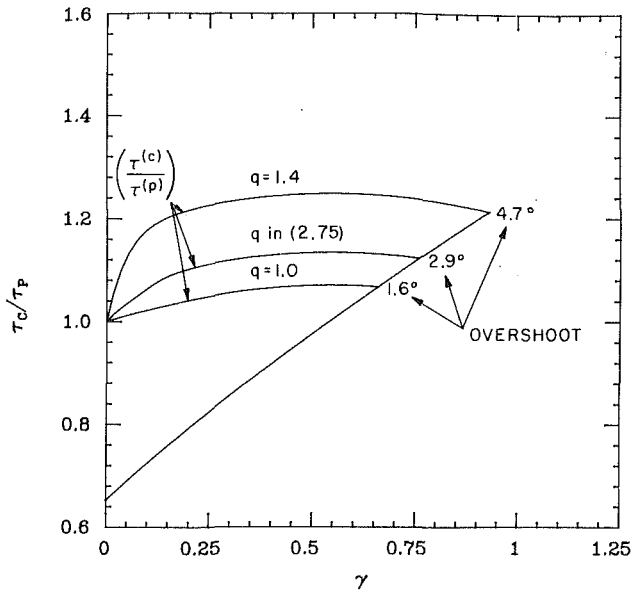

Fig. 3 This figure corresponds to simulations of single slip "overshoot" using the model of Fig. 2 for a rate-independent crystal. Various levels of latent hardening are indicated by the three values for q as explained in the text. The figure is taken from Peirce et al. [7].

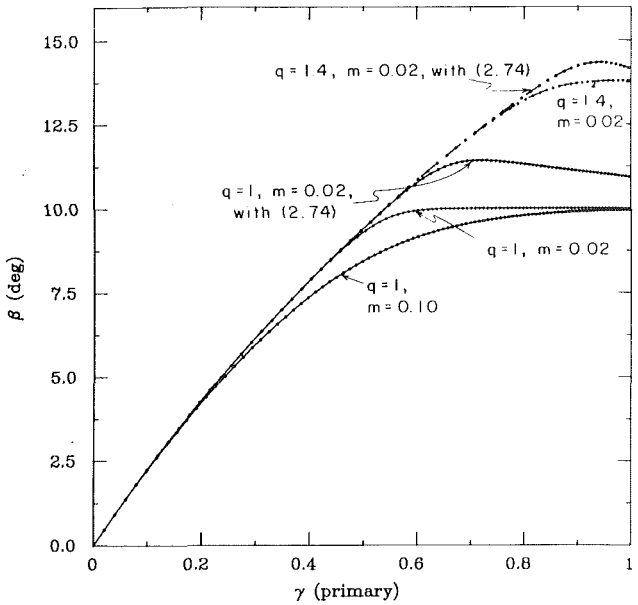

Fig. 4 Lattice rotation, β, and "overshooting" simulated using the planar model of Fig. 2 for a crystal deformed in tension. The crystal is rate-dependent and various strain-rate sensitivities, m, and levels of latent hardening, q, are indicated (taken from Peirce et al. [8]).

The calculations were performed for a rigid-plastic idealization of the crystal since the elasticity has a negligible effect on the lattice rotation. Kinematics links the angle of rotation β directly to the slip; at any stage for instance

$$\tan\beta = F^P_{12}/F^P_{22} \tag{2.77}$$

where $\mathbf{F}^P$ is the plastic part of the deformation gradient. The integration procedure is rather straightforward [2] and the results are shown in Figs. 3 and 4.

For the rate-independent crystal the hardening law given by (2.74) was used with

$$\mathcal{H}_{\alpha\beta} = qh + (1-q)\ h\ \delta_{\alpha\beta}. \tag{2.78}$$

q was varied between 1 and 1.4. As noted by Peirce et al. [7] the stress terms in (2.74) have the effect of contributing to latent hardening and overshoot. On the ordinate of Fig. 3 is plotted the ratio of the shear stresses on the conjugate and primary systems. The curves marked $(\tau^{(c)}/\tau^{(p)})$ are the ratios of the yield stresses plotted as functions of shear strain on the primary system. Note that even for $q=1$ the curve rises due to the aforementioned stress terms. The other line is the ratio of the resolved shear stresses generated on the slip systems by the tensile stress and it is presumed that when these two ratios are equal conjugate slip begins. At this point the net lattice rotation ceases due to conjugate slipping. The overshoot angles are listed on the figure where it is seen that the range of $1 \leq q \leq 1.4$ certainly does encompass the range of overshoot previously quoted.

For the rate-dependent calculation the hardening law was taken as (2.72) with $h(\gamma)$ again given by (2.76). The results, taken from the work of Peirce et al. [8], are shown in Fig. 4. In the figure, angle β is shown plotted as a function of the primary shear strain, γ; note that $\beta = 10$ deg corresponds to reaching a symmetric orientation.

When $q=1$ and the strain-rate sensitivity given by $m = 0.02$, the lattice rotation is such that $\beta \to 10$ deg and holds constant. In this case conjugate shearing comes on rather abruptly when the symmetry position is reached. When q is larger, e.g., $q=1.4$, overshoot of up to ~ 4 deg is evident as in the rate-independent case. One striking difference between the rate-independent and rate-dependent formulations is exemplified by the case where $q=1$ and $m=0.1$; a rather rate-sensitive case. Here the premature deviations from the curve for $q=1$ and $m=0.02$ are caused by earlier conjugate slip, that is, the flow law given by (2.70) allows conjugate slip to occur at a noticeable rate at resolved shear stress levels below that on the primary. Instances of such "undershooting" have indeed been observed in the literature. In fact, if q were larger than unity, initial undershoot would be followed by overshooting – again this type of behavior has been commonly observed.

Our tentative conclusion then is that levels of latent hardening ratios of 1-1.4 seem to account for a good deal of the observed data. Of course, the actual history of such ratios is undoubtedly quite complex so that even this rather approximate description can only be interpreted as an averaged effect on the hardening.

3 Analysis of Nonuniform Slip Phenomena in Single Crystals

An inevitable outcome of large strain plasticity in ductile solids is that homogeneous patterns of plastic flow break down into patterns characterized by nonuniform and highly localized plastic flow. The subject of localized deformation has received a good deal of attention during the past 10 years, largely because of the fundamental role it plays in limiting ductility and causing fracture. Analysis of localized deformation at large strains have shown the material's response is highly sensitive to constitutive description. For example, the existence of yield vertexes in rate-independent theories has been shown to promote bifurcations of a homogeneous deformation pattern into modes characterized by localized shear bands [21, 22]. An example of this for a single crystal is given in the following. Deviations from plastic normality, even when they are of such small magnitudes that are difficult to experimentally detect, likewise have been shown to promote the localization of plastic flow [6, 23].

There are, however, many other forms of nonuniform inelastic flow in crystalline materials, some catastrophic in their effects on ductility and others not, which are as yet unexplainied but clearly have important implications for the eventual development of large strain constitutive laws for

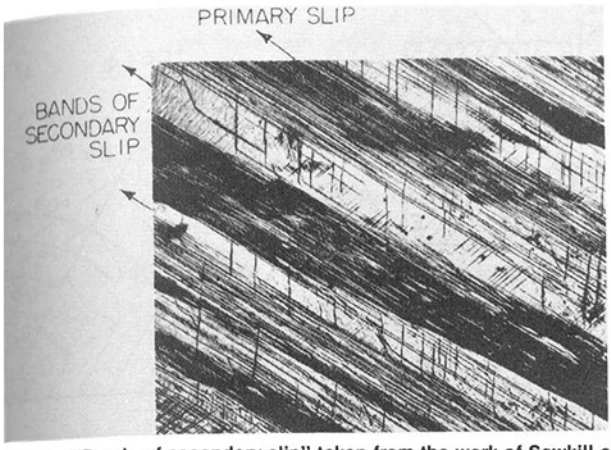

Fig. 5 "Bands of secondary slip" taken from the work of Sawkill and Honeycombe [24]

Fig. 6 An example of a discontinuous slip mode with the grains of polycrystalline aluminum, taken from Boas and Ogilvie [26]. The grain appears to break up into "patches," each characterized by a different mode of slip.

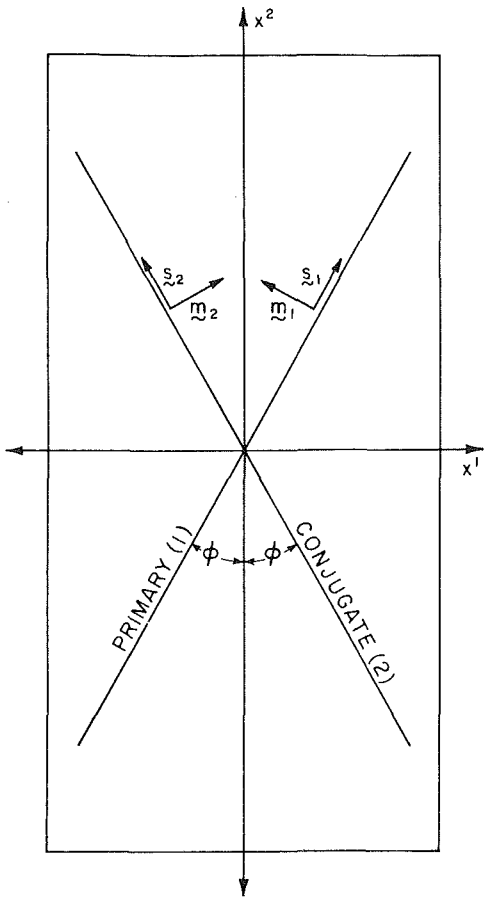

Fig. 7 Planar model for a single crystal subjected to tension. The crystal is presumed to undergo a primarily double mode of slip on the primary and conjugate slip systems.

polycrystals as well as single crystals. A case in point is illustrated in Fig. 5 which is taken from the work of Sawkill and Honeycombe [24]. As described by them, the (homogeneous) gage section of the crystal developed bands closely aligned with one slip system that were characterized by concentrated slip on other systems. These bands were referred to as "bands of secondary slip" and are kinematically quite different than the shear bands discussed by Chang and Asaro [25] and Peirce et al. [7, 8] in that they do not tend to accumulate very large strains. They do cause very significant lattice rotations and thus contribute to the development of nonuniform "texturing" of the crystal's gage section.

Another example of nonuniform slip is shown in Fig. 6 which is taken from the work of Boas and Olgivie [26]. In this case it is apparent that the *slip mode* within the individual grains of the polycrystal is nonuniform. The grains break up into what Peirce et al. [7] have called "patches," which are contiguous regions in which the slip modes are different. Since lattice rotation depends on the slip mode, the crystallographic orientation of neighboring patches becomes different which again leads to a nonuniform texture.

The development of nonuniform texture strongly affects the constitutive properties of the crystal. For one thing the kinematics of slip is changed to the point where it may no longer be sensible to refer to the specimen as a single crystal. The kinematics of slip is altered so that in some cases intensely localized deformation results. A case in point is the formation of shear bands resulting from "geometrical softening" or textural softening of the lattice studied by Chang and Asaro [25] and Peirce et al. [7]. In other cases macroscopically homogeneous deformation is promoted. For example, there are numerous examples of "contained bands" of localized deformation in both polycrystals and single crystals. By this is meant bands that are apparently constrained against propagating throughout the specimen's gage section. Peirce et al. [8] have illustrated how the orientation discontinuities associated with patchy slip in single crystals can prevent shear bands from propagating across patch boundaries. It is possible that similar geometric constraints act in polycrystals, but this has yet to be explored in sufficient depth.

We explore several examples of nonuniform flow in this section using the simple crystal model shown in Fig. 7 and the constitutive description just outlined.

In the interest of brevity, our attention is confined to rate-independent models; the reader is directed to other work for a discussion of rate dependence.

3.1 A Crystal Model. Since the kinematics of *nonuniform lattice rotation* require more than one slip system, complex slip phenomena described in the preceding section invariably occur when the slip mode is multiple slip. A simple plane model of a crystal undergoing a symmetric mode of primary-conjugate slip in tension is shown in Fig. 7. This model has been successfully used to describe the behavior of single crystals of common face-centered-cubic and body-centered-cubic models [2, 7]. As discussed in Section 2.4, crystals deformed in single slip undergo lattice rotations that eventually bring a second, i.e., the conjugate, slip system into a more or less symmetric orientation about the tensile axis with respect to the primary slip system. At this stage the deformation mode is predominantly double slip and the model geometry becomes applicable. There is, however, an im-

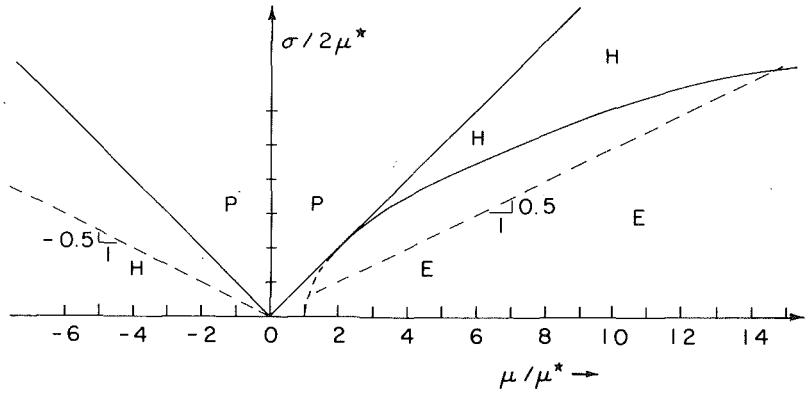

Fig. 8 Regimes of elliptic (*E*), parabolic (*P*), and hyperbolic (*H*) behavior of the equations governing the rate-independent crystal model shown in Fig. 7 (taken from Peirce et al. [8])

portant proviso: although at any stage in a program of homogeneous deformation the model geometry makes both slip systems critical, there is still the question of what will be the slip mode in the next increment of loading. If the slip mode is nonunique, as it may well be in the rate-independent idealization, then so is the rotation of the lattice relative to the material. The description of texturing is therefore nonunique and a proper description of slip phenomena becomes impossible. In the next section a bifurcation analysis is presented which is based on an assumed mode of double slip of a rate-independent crystal. This analysis is very helpful in uncovering the origins of the sort of nonuniform slip phenomena described in the foregoing. However, as noted by Asaro [2] and more specifically by Peirce et al. [8] the kinematic uncertainties of rate independence preclude a full analysis, at least if a reasonably complete set of material parameters is used. To gain some specific understanding of this, the slip-mode uniqueness question for the model of Fig. 7 is examined first. This is done using the sufficiency conditions given by Hill and Rice [4].

For reasons to be explained in the next section, it is instructive to take the elasticity of the model crystal shown in Fig. 7 to be isotropic and incompressible. In this case the matrice elements of $\mathbf{g}$ and $\mathbf{k}$ take the form

$$\mathbf{g}_{\alpha\beta} = h_{\alpha\beta} - (\sigma/2)\cos 2\phi + G,\ \alpha = \beta \tag{3.1$_1$}$$

$$\mathbf{g}_{\alpha\beta} = h_{\alpha\beta} + (\sigma/2)\cos 2\phi - G\cos 4\phi,\ \alpha \neq \beta \tag{3.1$_2$}$$

and

$$k_{\alpha\beta} = h_{\alpha\beta} + (\sigma/2)\cos 2\phi + \mathcal{O}(\sigma^2/G),\ \alpha = \beta \tag{3.2$_1$}$$

$$k_{\alpha\beta} = h_{\alpha\beta} - (\sigma/2)\cos 2\phi + \mathcal{O}(\sigma^2/G),\ \alpha = \beta \tag{3.2$_2$}$$

We also recall that when the deformation rates are specified, slip-mode uniqueness is guaranteed if $\mathbf{g}$ is positive-definite; when the $\overset{\nabla}{T}$'s are specified uniqueness follows when $\mathbf{k}$ is positive-definite.

If the degenerate case of $\phi = \pi/4$ is excluded, it is clear that so long as σ and the $h_{\alpha\beta}$ are much less than G, $\mathbf{g}$ is positive-definite. The situation is quite different when the stress rates are specified as noted by Pan and Rice [16]. If, for example, we take $h_{11} = h_{22} = h$ and $h_{12} = h_{21} = h_1$ as the model's orthotropic symmetry might imply we find that $\mathbf{k}$ is positive-definite if and only if

$$h - h_1 + \sigma\cos 2\phi > 0 \tag{3.3}$$

or if we set $h_1 = qh$ as in the discussion of Section 2.6, if

$$(\sigma/h)\cos 2\phi > (1-q). \tag{3.4}$$

In Section 2.4, it was noted that experimental observations easily incorporate the range $1 \leq q \leq 1.4$ for latent hardening. If q is set at 1.4 and ϕ at 30 deg to model on face-centered-cubic crystal as in Asaro [2] and Peirce et al. [7, 8] the inequality (3.4) becomes $\sigma/h > 0.8$ or, since the resolved shear stress on either slip system is $\tau = \sigma/2 \sin 2\phi = 0.43\,\sigma$, $\tau/h > 0.346$. There are numerous cases where this inequality would fail – in fact it would fail during the first 1 percent strain of almost any ductile metal single crystal. If $\phi > \pi/4$, $\cos 2\phi < 0$ and uniqueness requires $q < 1$ which is effectively ruled out by experiment. When more realistic models for crystals are examined, e.g., with 12 slip systems for face-centered-cubic crystals, uniqueness is even more difficult to guarantee in either case, and the range of possible geometries and strain hardening required to do so is too restrictive to include real materials. This, incidentally, has been one of the major difficulties in the prediction of deformation texture in polycrystals. Nonetheless, considerable progress can be made using the rate-independent model. The reader is referred to the work of Peirce et al. [8] for a discussion of their rate-dependent formulation which overcomes these limitations and allows the complete range of material properties to be included.

3.2 Bifurcation Phenomena and Slip Patterns. When the crystal's elasticity is taken as isotropic and incompressible, the crystal model falls into the class of plane orthotropic incompressible solids studied by Biot [27] and Hill and Hutchinson [28]. In particular, the rather comprehensive bifurcation analysis presented by Hill and Hutchinson [28] applies. The constitutive laws take the form

$$\overset{\nabla}{\sigma}_{22} - \overset{\nabla}{\sigma}_{11} = 2\mu^*(D_{22} - D_{11}) \tag{3.5}$$

$$\overset{\nabla}{\sigma}_{12} = 2\mu\, D_{12} \tag{3.6}$$

with the condition of incompressibility expressed as

$$D_{11} + D_{22} = 0. \tag{3.7}$$

The two instantaneous moduli μ and μ^* are defined so that μ governs shear parallel to the x_1, x_2 coordinate axes and μ governs shear at 45 deg to them. With this in mind it is clear that when $\phi = \pi/4$, μ is essentially the elastic modulus since simple shearing on the slip systems does not produce shear parallel to the x_1, x_2 coordinate axes. When ϕ differs from $\pi/4$ shear involves plastic straining and the material's stiffness rapidly decreases. This is equivalent to the formation of a yield vertex and development of vertex softening.

The moduli μ and μ^* are (see Asaro [2] or Peirce et al.)

$$\mu^* = \frac{Gh^*(1+q)}{h^*(1+q) + 2G\sin^2 2\phi^*} \tag{3.8}$$

and

$$\mu = \frac{G(h^*(1-q) + \sigma\cos 2\phi^*) - \sigma^2/2}{h^*(1-q) + 2G\cos^2 2\phi^* - \sigma\cos 2\phi^*} \tag{3.9}$$

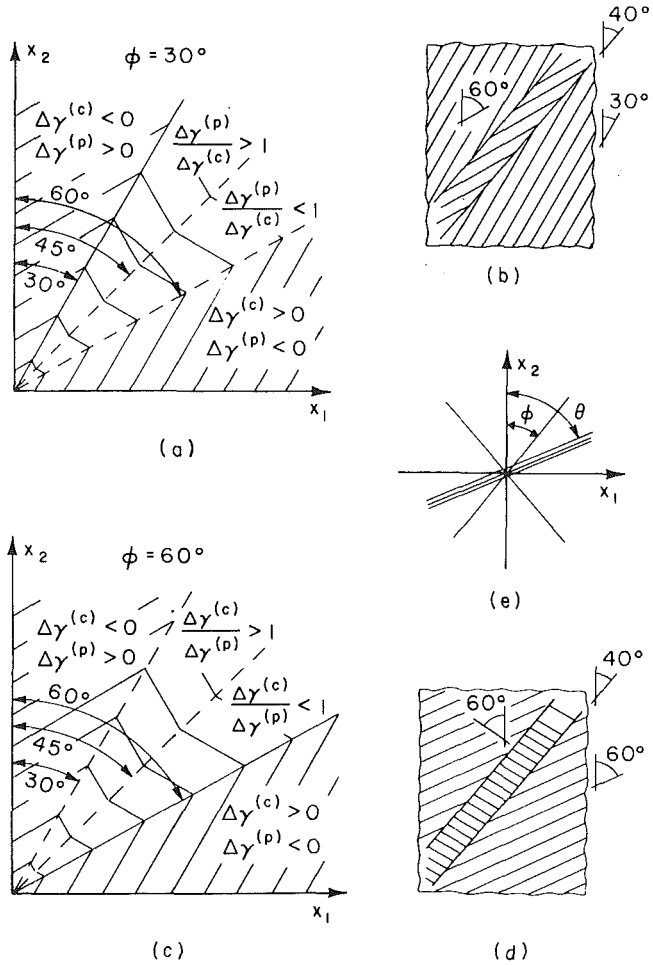

Fig. 9 Slip patterns and loading regimes for the localized bands of slip described in the text (taken from the work of Peirce et al. [8])

where the moduli $h_{\alpha\beta}$ are taken so that $h_{11} = h_{22} = h$ and $h_{12} = h_{21} = h_1 = qh$. h^* and ϕ^* are elastically altered quantities,

$$h^*\left(\frac{ds^*}{ds}\right) = h \tag{3.10}$$

and

$$\lambda^{*2}\tan\phi^* = \tan\phi \tag{3.11}$$

where ds^*/ds is the elastic stretch ratio of either slip direction and λ^* is the elastic stretch ratio along the tensile axis. For practical purposes (i.e., when σ/G, $h/G << 1$) the elastic terms can be set aside and then

$$\mu^* = \frac{h(1+q)}{2\sin^2 2\phi} \tag{3.12}$$

and

$$\mu = \frac{h(1-q)+\sigma\cos 2\phi}{2\cos^2 2\phi}. \tag{3.13}$$

In what follows we examine the conditions that allow the deformation mode to bifurcate into bands of localized deformation. As shown by Hill and Hutchinson [28] for a band to form with unit normal **n** continuing equilibrium and compatability require that

$$(\mu - 1/2\sigma)n_1^4 + 2(2\mu^* - \mu)n_1^2 n_2^2 + (\mu + 1/2\sigma)n_2^4 = 0. \tag{3.14}$$

The governing equations are elliptic, parabolic, or hyperbolic depending on whether there are 0, 2, or 4 real solutions for n_2/n_1. Figures 8 and 9, taken from the recent work of Peirce et al. [8], summarize the bifurcation results and the kinematics of the localized bands that form. The coordinates in Fig. 8 are given by

$$\mu/\mu^* = \frac{[(1-q)+(\tau/h)\cot 2\phi]\tan^2 2\phi}{(1+q)} \tag{3.15}$$

and

$$\mu/2\mu^* = \frac{(\tau/h)\sin 2\phi}{(1+q)} \tag{3.16}$$

where we note $\sigma/2\mu^* > 0$ so long as h and q are positive.

When this model is applied to face-centered-cubic crystals undergoing tension, ϕ is set equal to 30 deg. Now as pointed out by Peirce et al. [8], if $q = 1$, $(\sigma/2\mu^*)/(\mu/\mu^*) = 0.5$ and the trajectory is along the line of slope 0.5 indicated in Fig. 8. When this line intersects the *E-H* boundary there are two *coincident* sets of real characteristics; the angles θ_1 and θ_2 that make the tensile axis are in the range 38–40 deg. What is also apparent from Fig. 8 is that the ratio of σ/h (generally referred by its inverse h/σ) at this point is *positive* and equal to approximately $(h/\sigma)_{crit} \approx 0.04$. This indicates, as noted earlier, that localized flow is possible in defect-free crystals with *positive strain hardening* and that strain softening is not necessary. At other values of q, say in the range $0 \le q \le 2$, the results are quite similar with h/σ in the range $0.03 \le (h/\sigma)_{crit} \le 0.06$.

Figure 9 indicates that the bands just described involve predominantly shear on the slip system to which they are nearly parallel; this is referred to as the primary slip system. In general if the bands are taken to be a simple shearing mode, and are inclined by the angle θ to the tensile axis, the ratio of excess straining on the primary to that on the congugate system is

$$\frac{\Delta\gamma^{(p)}}{\Delta\gamma^{(c)}} = \frac{\sin 2(\theta+\phi)}{\sin 2(\theta-\phi)}. \tag{3.17}$$

On the other hand, it is also possible to show that the net *lattice* spin rate in the band is

$$\Omega_{12}^* = 1/2\left(1 - \frac{\cos 2\theta}{\cos 2\phi}\right)\dot{\gamma} \tag{3.18}$$

where $\dot{\gamma}$ is the net shearing rate in the band. If $\theta \approx 40$ deg with $\phi \approx 30$ deg, $\Omega_{12}^* > 0$ and lattice tends to rotate *away* from the tensile axis. This has the effect of increasing the Schmid stress on the primary system and promoting additional slip. In other words as the slip direction rotates from an initial angle of 30 deg *toward* the maximum shear stress 45 deg orientation, the dominant slip system becomes "geometrically softened." This is an example of a textural softening effect that leads to highly localized and potentially unstable flow.

When $\phi = 60$ deg in this model a rather different nonuniform mode appears. If we again take $q = 1$ for illustration we find $\mu/\mu^* < 0$, $(\sigma/2\mu^*)/(\mu/\mu^*) = -0.05$, and the trajectory is along the line of slope -0.05 in the hyperbolic regime. Now during a typical program of straining the magnitude of μ/μ^* increases and Peirce et al. [8] have shown that as $\mu/\mu^* \to -\infty$, $\theta_1 \to 45$deg and $\theta_2 \to 60$ deg; when $\mu/\mu^* > -2.0$, $\theta_1 < 30$ deg and $\theta_2 > 60$ deg. Figure 9 shows, therefore, that the first bands to appear, which are characterized by active loading on both systems, have orientations 30 deg $\le \theta \le$ 45 deg and are dominated by conjugate slip. The lattice rotations specified by (3.18) would in this case indicate that eventually the conjugate system becomes geometrically hardened (after an initial softening) whereas the Schmid stress on the primary system becomes negligible and may indeed vanish. Thus this mode will not tend to accumulate arbitrarily large strains.

The slip patterns expected from these two modes are sketched in Fig. 9. The shear band modes predicted when $\phi =$ 30 deg are known to compare to shear bands found ex-

perimentally in face-centered-cubic crystals. Lattice rotations that produce geometrical or textural softening have been documented [25, 2]. For the modes corresponding to "bands of secondary slip" the comparison is only qualitative at present, but the slip pattern does resemble that shown earlier in Fig. 5.

One of the more striking aspects of the phenomena just described is their dependence on lattice kinematics. The development of texture and the softening or hardening associated with it depends on the precise specification of the slip mode. If this is not uniquely specified a detailed analysis becomes impossible. As pointed out in Section 2.6, slip-mode uniqueness is generally difficult to guarantee when a full range of material properties are used and for this reason it appears that a full analysis of slip phenomena in crystals undergoing multiple slip will not be possible within a rate-independent framework. Peirce et al. [8] have now extended the theory to incorporate rate-dependent material behavior and have carried out finite element calculations of nonuniform and localized flow in single crystals. The reader is directed to their work for further details.

4 A Direction for Future Research

One of the more important outstanding problem areas in crystalline plasticity is the development of models for large strain deformation of polycrystals. The need for this has been made clear in recent years, especially in connection with studies of nonuniform and unstable deformation. For example, the softening effects produced by yield vertexes in rate-independent plasticity in response to nonproportional stressing have been shown to promote localized plastic flow in cases where homogeneous flow would otherwise be expected [21, 2, 23]. It is well known that micromechanical models for crystalline slip such as presented in the previous sections lead to vertex structure for polycrystals even at small strains [9, 18]. What has not been explored in near sufficient detail, however, are the very important effects of deformation-induced anisotropy on material stiffness at large strains. A promising, albeit challenging, direction, therefore, is the extension of the micromechanical theory outlined in the foregoing to a description of polycrystalline plasticity at large strains. A vital feature of such models should be the description of deformation-induced anisotropy, and ultimately a proper description of phenomena occurring at grain boundaries.

One important cause of anisotropy is the formation of crystallographic texture. In his now classic treatment of axisymmetric tension in face-centered-cubic polycrystals, Taylor [3] described how the slip-induced rotation of the lattice within the grains caused a <111> – <100> "fiber" texture to develop in aggregates with an initially *uniform* array of grain orientations. That is, the grains in an initially isotropic aggregate tend to take on crystallographic orientations that align either a <111> or <100> type crystallographic direction with the tensile axis. Taylor's original analysis has been the inspiration and conceptual foundation of a broad range of further experimental and theoretical study of texture in metal polycrystals [29]. Nearly all of the work, however, has been confined to small strains and thus provides only suggestions of the vital influences texture has on material behavior at large strains. What is suggested, on the other hand, appears of sufficient importance to warrant a considerable new effort. In closing, an example of some intriguing and evidently important strain-hardening phenomenology is outlined.

Effect of Texture on Strain Hardening. As mentioned in the foregoing, there is a widespread interest in documenting and describing material strain-hardening at large strains. For this purpose experimental techniques such as wire drawing and torsion testing are commonly used to avoid the inherent instabilities of simple tension tests [30]. What is commonly observed, however, is that the flow stresses and strain-hardening rates measured in torsion are much less than those extracted from tension tests. Examples of this have recently been given by Shrivastava et al. [31] who suggest that deformation texture accounts for a good part of the observed effect.

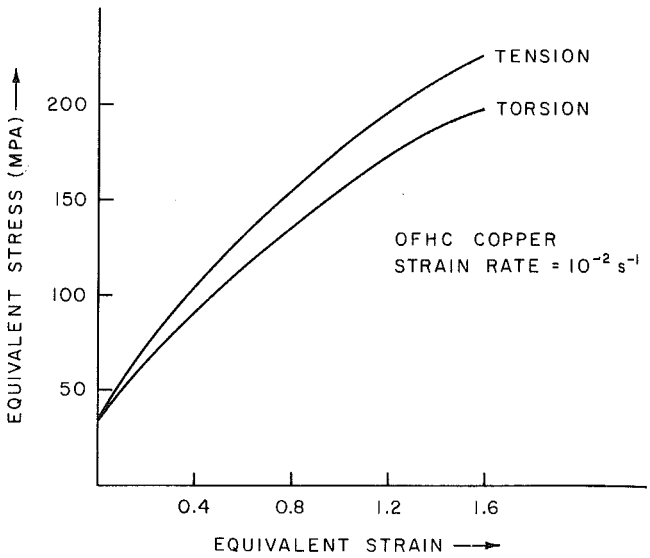

Fig. 10 Strain-hardening curves for copper as extracted from separate torsion and tension tests. The curves are taken from the paper by Shrivastava et al. [31] who conclude that torsion is characterized by a lower strain-hardening rate than tension.

Figure 10 shows a comparison of strain-hardenig curves for single-phase polycrystalline copper taken from the work of Shrivastava et al. [31]. The curves are compared in the basis of equivalent stress versus what they define as equivalent strain. The equivalent stress is defined as

$$\sigma_{eq} = \sqrt{3J_2} \tag{4.1}$$

where J_2 is the second invariant of deviatoric Cauchy stress. Equivalent strain was computed by integrating the expression for the increment in equivalent strain, defined as in (4.1) but multiplied by a factor of 2/3 with the invariant of strain deviator replacing J_2, along the entire strain path. In this way Shrivastava et al. [31] established a correspondence between torsion and simple shear in that $\epsilon_{eq} = \gamma\sqrt{3}$ in both cases. For the tension test they took $\epsilon_{eq} = ln\ \lambda_1$ where λ_1 is the stretch along the tensile axis. The difference between the tension and torsion strain-hardening curves shown for this example is representative for a wide range of face-centered-cubic metals. Furthermore, although it may be argued that presenting data in terms of these particular equivalent quantities is arbitrary, the effect illustrated is qualitatively common to other strain measures.

Shrivastava et al. [31] suggest that the role of texture may be seen as follows. For an isotropic face-centered-cubic polycrystal deformed in axisymmetric tension, Taylor [3] had shown that the average ratio of cumulative shear-strain increments on the active slip systems to the increment of principal tensile strain was approximately 3.06. Taylor's model was rigid plastic and based on the assumption that all grains were subject to the *same axisymmetric strain increment*. This latter aspect of the model is often overlooked, by the way. The procedure of imposing axisymmetric strain increments to simulate a tension test requires justification, and in Taylor's specific calculation, this was provided by the additional assumption of initial isotropy of the aggregate.

Taylor's calculations were confined to a neighborhood around initial yield and indicated only the initial trends in grain rotation and texture development. The result of his analysis is that if τ_c is the slip-plane yield stress, common to all slip systems, the tensile yield stress is $\sigma = 3.06\,\tau_c$. With the adopted definition of equivalent stress this yields $\sigma_{eq}^{yT} = 3.06\,\tau_c$. Bishop and Hill [32] later extended the Taylor model to yielding of polycrystals comprised of rigid-plastic grains subjected to multiaxial loading and found that for initially isotropic face-centered-cubic polycrystals the yield strength in shear was approximately $1.65\,\tau_c$. Again with the definition of equivalent stress adopted in the foregoing, this means that $\sigma_{eq}^{ys} = 1.65\sqrt{3}\,\tau_c = 2.86\,\tau_c$. Thus with the understanding that these models yield upper-bound approximations to the actual yield strengths, the yield strength in torsion is expected to be some 6.5 percent lower than in tension.

Now the numbers 3.06 and 1.65 have come to be known in the metallurgical literature as average Taylor factors. They are computed for each grain by imposing the aggregate strain and determining the active slip systems and the amounts of shear on each of them in accordance with isotropic hardening and Taylor's [3] minimum work principal or equivalently Bishop and Hill's [32] maximum work postulate. For axisymmetric tension, for example, the Taylor factor equals 3.674 for a face-centered-cubic grain aligned with a <111> direction along the tensile axis and 2.449 for a grain aligned along a <100> direction. To the extent that the aggregate remains transversely isotropic it is found that the fiber texture described earlier tends to increase the average value of this factor above the isotropic aggregate value of 3.06 thereby causing a textural hardening. Another way of appreciating this is by noting that the so-called Taylor factor represents the ratio of the cumulative shear-strain increment on the active slip systems to the maximum principal strain increment produced by the slips. Qualitatively, then, the lower the value of the Taylor factor the less total slip is required to produce the imposed strain increment. When the strain hardening is approximately isotropic a similar comment may be made concerning the strain-hardening increment, $d\tau_c$. The situation is somewhat different for torsion.

At finite strains the texture developed in torsion can be described as composed of three principal comonents which involve placing {111}, {112}, or {101}-type crystal planes in the plane of shear and, respectively, <112>, <111>, or <110>-type directions parallel to radial directions. Citing Shrivastava et al. [31], this has the effect of slightly reducing the average Taylor factor from the Bishop and Hill value of 1.65 which leads to a textural softening. Furthermore a qualitative study of the slip mode in these two cases indicates that in tension, the strong <111> texture component in materials like copper involves the activation of possibly six slip systems (as judged within the rate-independent theory) while in torsion the stronger {111} component described in the foregoing would involve only one slip system. For the other texture components the situation is similar in that tension involves slip on many systems while in torsion only one or two are active. The point here is made most effectively by calling to mind the discussion of Section 2.6 on latent hardening and by extrapolating our discussion a bit beyond the Taylor model.

Taylor's calculatons were based on the assumption of isotropic hardening i.e., $q = 1$ (cf Section 2.6). Experimental observations suggest that q is larger than 1 for systems whose slip planes intersect. Thus the operation of six or eight systems in the case of axisymmetric tension should involve a greater increment in strain hardening (i.e., the increase in τ_c) for a given cumulative shear strain than for the corresponding case in torsion. Thus there are two effects proposed here, both strongly kinematical in nature: the first is that simple shear (identified with torsion) has a lower net Taylor factor than axisymmetric tension, which means that for a given increment of equivalent strain, a smaller increment in cumulative glide strain is required; the second is simple shear involves the operation of fewer intersecting slip systems and should accordingly be characterized by a reduced overall strain-hardening rate.

There is little value in pursuing this speculative line much further in the context of small strain-rate-independent models such as the Taylor model. For one thing, the kinematical nonuniqueness associated with rate independence renders clear cut analyses of texture development itself impossible, especially when realistic descriptions of latent hardening are included. In addition, there are other cautions concerning the interpretation of experimental data that must be born-in mind in pursuing future study. For example, the preceding discussion has been concerned with the possible, or perhaps likely, role of deformation-induced crystallographic texture. There is also the matter of texturing of the material itself, involving inter alia the elongating and flattening of grains. In a rate-dependent formulation the slip mode is unique but dependent on stress state. Gross alterations in grain shape would affect the manner in which neighboring grains interact and thereby affect the slip modes. Similar complications arise no doubt from very fine grain size. Neither of these have as yet been included in polycrystalline models.

Polycrystalline models developed to data fall within two broad categories. First is the Taylor isostrain type as extended by Bishop and Hill [32] for rate-independent materials and by Hutchinson [15] for rate-dependent (but small strain) creep. The second is the class of self-consistent models, in particular as proposed by Hill [33], and again used by Hutchinson [15] for time-dependent materials deforming by steady-state power law creep. In either case rate dependence and the slip-mode uniqueness it imparts would appear to be vital to produce a well-posed kinematical structure so that texture evolution may be unambiguously predicted. In addition, the models used to study texture development should not be based on a priori prescribed strain increments as in the Taylor model. Typical (homogeneous) deformation processes would specify some of the strain rates and other (nonconjugate) stress rates. For example, a model for a simiple tension test might specify the axial strain rate, possibly the *orientation* of the principal tensile fiber, and vanishing transverse stresses. Models of this type could be used, for example, to assess the effects of tension on the development of textural softening in shear, on whether this leads to significantly reduced softening with respect to nonproportional stressing, and if this would promote unstable or localized flow. In this regard we note that Dillamore and coworkers [34] have reported experimental evidence that localized shear bands in polycrystals are characterized by textural softening.

Acknowledgments

This manuscript was prepared with the support of the Brown University Materials Research Laboratory funded by the U. S. National Science Foundation. The collaboration and many fruitful discussions I have had with A. Needleman and J. R. Rice dealing with the mechanics of crystals are also gratefully acknowledged.

References

1 Argon, A. S., ed., *Constitutive Equations in Plasticity*, MIT Press, Cambridge, Mass., 1975.

2 Asaro, R. J., "Micromechanics of Crystals and Polycrystals," in *Advances in Applied Mechanics*, Vol. 23, Academic Press, in press.

3 Taylor, G. I., "Plastic Strain in Metals," *J. Inst. Metals*, Vol. 62, 1938, pp. 307-324.

4 Hill, R., and Rice, J. R., "Constitutive Analysis of Elastic-Plastic Crystals at Arbitrary Strain," *J. Mech. Phys. Solids*, Vol. 20, 1972, pp. 401-413.

5 Hill, R., "Generalized Constitutive Relations for Incremental Deformation of Metal Crystals by Multislip," *J. Mech. Phys. Solids*, Vol. 14, 1966, pp. 95-102.

6 Asaro, R. J., and Rice, J. R., "Strain Localization in Ductile Single Crystals," *J. Mech. Phys. Solids*, Vol. 25, 1977, pp. 309-338.

7 Peirce, D., Asaro, R. J., and Needleman, A., "An Analysis of Nonuniform and Localized Deformation in Ductile Single Crystals," *Acta Metall.*, Vol. 30, 1982, pp. 1087-1119.

8 Peirce, D., Asaro, R. J., and Needleman, A., "Material Rate Dependence and Localized Deformation in Crystalline Solids," in press.

9 Hill, R., "The Essential Structure of Constitutive Laws for Metal Composites and Polycrystals," *J. Mech. Phys. Solids*, Vol. 15, 1966, pp. 79-95.

10 Rice, J. R., "On the Structure of Stress-Strain Relations for Time-Dependent Plastic Deformation in Metals," ASME JOURNAL OF APPLIED MECHANICS, Vol. 37, 1970, pp. 728-737.

11 Rice, J. R., "Inelastic Constitutive Relations for Solids: An Internal-Variable Theory and its Application to Metal Plasticity," *J. Mech. Phys. Solids*, Vol. 19, 1971, pp. 433-455.

12 Hill, R., and Rice, J. R., "Elastic Potentials and the Structure of Inelastic Constitutive Laws," *SIAM, J. Appl. Math.*, Vol. 25, 1973, pp. 448-461.

13 Hill, R., "On Constitutive Inequalities for Simple Materials," *J. Mech. Phys. Solids*, Vol. 16, 1968, pp. 229-242; pp. 315-322.

14 Hill, R., "Aspects of Invariance in Solid Mechanics," in *Advances in Applied Mechanics*, Vol. 18, 1978, pp. 1-75.

15 Hutchinson, J. W., "Bounds and Self-Consistent Estimates for Creep of Polycrystalline Materials," *Proc. Roy. Soc.*, Series, A, Vol. 348, 1976, pp. 101-127.

16 Pan, J. and Rice, J. R., unpublished research, Brown University, 1981.

17 Kocks, U. F., "The Relation Between Polycrystalline Deformation and Single-Crystal Deformation," *Metall. Trans.* Vol. 1, 1970, pp. 1121-1142.

18 Hutchinson, J. W., "Elastic-Plastic Behavior of Polycrystalline Metals and Composites," *Proc. Roy. Soc.*, Series A, Vol. 319, 1976, pp. 247-272.

19 Hill, R., "A General Tehory of Uniqueness and Stability in Elastic-Plastic Solids," *J. Mech. Phys. Solids*, Vol. 6, 1958, pp. 236-249.

20 Havner, K. S., and Shalaby, A. H., "A Single Mathematical Theory of Finite Distortional Latent Hardening in Single Crystals," *Proc. Roy. Soc.*, Series A, Vol. 358, 1977, pp. 47-70.

21 Rice, J. R., "The Localization of Plastic Deformation," in *Proceedings of 14th International Congress of Theoretical and Applied Mechanics*, I, North-Holland, 1977.

22 Hutchinson, J. W., and Tvergaard, V., "Surface Instabilities on Statistically Strained Plastic Solids," *Int. J. of the Mech. Sci.*, Vol. 22, 1980, pp. 339-354.

23 Needleman, A., and Rice, J. R., "Limits to Ductility Set by Plastic Flow Localization," in *Mechanics of Sheet Metal Forming*, Koistinen, D. P., and Wang, N. M., eds., Plenum Press, New York, 1978, pp. 237-

24 Sawkill, J., and Honeycombe, R. W. K., "Strain Hardening in Face-Centered Cubic Metals Crystals," *Acta Metal.*, Vol. 2, 1954, pp. 854-864.

25 Chang, Y. W., and Asaro, R. J., "An Experimental Study of Shear Localization in Aluminum-Copper Single Crystals," *Acta Metal.*, Vol. 29, 1981, pp. 241-257.

26 Boas, W., and Ogilvie, G. J., "The Plastic Deformation of a Crystal in a Polycrystalline Aggregate," *Acta Metall.*, Vol. 2, 1954, pp. 655-659.

27 Biot, M., *Mechanics of Incremental Deformations*, Wiley, New York, 1965.

28 Hill, R., and Hutchinson, J. W., "Bifurcation Phenomena in Plane Strain Tension Test," *J. Mech. Phys. Solids*, Vol. 23, 1975, pp. 239-264.

29 Gil Sevillano, J., van Houtte, P., and Aernoudt, E., "Large Strain Work Hardening and Textures," *Progress in Materials Science*, Vol. 25, 1980, pp. 69-412.

30 Hecker, S. S., Stout, M. G., and Eash, D. T., "Experiments on Plastic Deformation at Finite Strains," in *Plasticity of Metals at Finite Strain*, Lee, E. H., and Mallett, R. L., eds., Stanford Univ. Publ., 1982, pp. 162-205.

31 Shrivastava, S. C., Jonas, J. J., and Canova, G., "Equivalent Strain in Large Deformation Torsion Testing: Theoretical and Practical Considerations," *J. Mech. Phys. Solids*, Vol. 30, 1982, pp. 75-90.

32 Bishop, J. F. W., and Hill, R., "A Theoretical Derivation of the Plastic Properties of a Polycrystalline Face-Centered Metal," *Philos. Mag.*, Vol. 42, 1951, pp. 414-427.

33 Hill, R., "A Self-Consistent Mechanics of Composite Materials," *J. Mech. Phys. Solids*, Vol. 13, 1965, pp. 213-222.

34 Dillamore, I. L., Roberts, J. G., and Bush, A. C., "Occurrence of Shear Bands in Heavily Rolled Cubic Metals," *J. Metal Sci.*, Vol. 13, 1979, pp. 73-77.